

Yu.F.Baranov, C.D.Challis, J. Hobirk, M.Baruzzo, T. Hender
and JET EFDA contributors

Interplay Between Confinement, Impurities and MHD in JET Hybrid Pulses with ITER-like Wall

Interplay Between Confinement, Impurities and MHD in JET Hybrid Pulses with ITER-like Wall

Yu.F.Baranov¹, C.D.Challis¹, J. Hobirk², M.Baruzzo³, T. Hender¹
and JET EFDA contributors*

JET-EFDA, Culham Science Centre, OX14 3DB, Abingdon, UK

¹*EURATOM-CCFE Fusion Association, Culham Science Centre, OX14 3DB, Abingdon, OXON, UK*

²*Max-Planck-Institut für Plasmaphysik, EURATOM Association, Boltzmannstr. 2, 85748 Garching*

³*Consorzio RFX, EURATOM-ENEA Association, Corso Stati Uniti 4, 35127 Padova, Italy*

** See annex of F. Romanelli et al, "Overview of JET Results",
(24th IAEA Fusion Energy Conference, San Diego, USA (2012)).*

Preprint of Paper to be submitted for publication in Proceedings of the
40th EPS Conference on Plasma Physics, Espoo, Finland.

1st July 2013 – 5th July 2013

“This document is intended for publication in the open literature. It is made available on the understanding that it may not be further circulated and extracts or references may not be published prior to publication of the original when applicable, or without the consent of the Publications Officer, EFDA, Culham Science Centre, Abingdon, Oxon, OX14 3DB, UK.”

“Enquiries about Copyright and reproduction should be addressed to the Publications Officer, EFDA, Culham Science Centre, Abingdon, Oxon, OX14 3DB, UK.”

The contents of this preprint and all other JET EFDA Preprints and Conference Papers are available to view online free at www.iop.org/Jet. This site has full search facilities and e-mail alert options. The diagrams contained within the PDFs on this site are hyperlinked from the year 1996 onwards.

ABSTRACT.

High confinement improvement (H-factor) relative to the IPB98(y,2) scaling law [1], stability and β_N are achieved in JET hybrid scenario pulses due to formation of specific safety factor (q) profiles with broad flat region around $q \sim 1$ in the plasma core and steep dq/dr at the edge. The replacement of the C-wall with Be/W-wall caused changes in the impurity content with effect on the q-profile, MHD, radiation and τ_E . An interaction between these factors in hybrid pulses with ILW has been analysed using transport modelling and important statistical tendencies identified.

1. CONFINEMENT EVOLUTION.

Some optimisation has been done for hybrid plasmas with ILW to recover the required q-profile shape and plasma performance of the C-wall hybrid scenario. There is a collinearity between maximum reached confinement improvement H-factor and maximum reached β_N in hybrid pulses with ILW with $\max(\beta_N)$ factor varying from 1.5 to 3.5 and $\max(H)$ rising from ~ 0.85 to 1.35. $\max(\beta_N)$ and $\max(H)$ were reached almost simultaneously in every pulse during, typically, first 1.5-2s of the high power phase. However, quasi-steady state regime could not be sustained in contrast to C-wall plasmas. The rate of confinement degradation is shown in fig.1 as a function of maximum reached H for every hybrid pulse with ILW. The dependence of the confinement degradation ΔH on maximum β_N looks very similar to Fig.1 if $\max H$ axis is replaced by $\max \beta_N$. The larger $\max(\beta_N)$ reached the stronger is the confinement degradation ΔH . The H-factor decreases to 1.1 or smaller value typically in 1-2.5s from its maximum. Very small variation in H or β_N has been observed in pulses with low $\max(\beta_N) < 2$ or $\max(H) < 1.1$.

2. IMPURITIES AND RADIATION

Significant increase in Z_{eff} is observed in hybrid pulses with ILW as shown in Fig.2. $Z_{\text{eff}} = (Z_{\text{effH}} + Z_{\text{effV}})/2$ is deduced from Bremsstrahlung emission measured along horizontal (Z_{effH}) and vertical (Z_{effV}) lined of sight as shown in fig.3. The plasma radiation becomes peaked (Fig.4) as measured by horizontal bolometer camera. Soft X-ray emission profiles are qualitatively similar to the radiation profiles. Radiation and SXR emission profiles measured by vertical cameras in pulses with good confinement ($H > 1.1$) show that the maximum of the radiation is around equatorial plane and shifted from the magnetic axis to the low magnetic field side. Such shift is associated with effect of centrifugal force on the heavy impurities due to strong toroidal plasma rotation. In some cases the radiation peak moves to the centre. The radiation peaking is associated with peaking of the heavy impurity profiles. The horizontal line of sight for Z_{effH} measurement is aligned with the max of radiation and impurity concentration and the vertical line of sight (Z_{effV}) is misaligned. There is a strong correlation between the radiation peaking and $Z_{\text{effH}} - Z_{\text{effV}}$ as shown in Fig.5 due to misalignment of Z_{eff} maximum and Z_{effV} line of sight. Light (Be) and heavy impurity (W, Ni) accumulation has been modelled using Jetto-Sanco codes, matching measured radiation, soft X-ray emission and $Z_{\text{effH}} = Z_{\text{eff}}$ measured along the horizontal line of sight (Fig.3). The model used includes the neoclassical

velocity and diffusivity inside the edge barrier and anomalous Bohm-gyro-Bohm diffusivity in the core. Anomalous pinch velocity ($V_a \sim 1 \text{ m/s} > V_{neo}$) was required to reproduce the observed peaked radiation profiles in the phase of rising β_N , when the plasma density in the core is flat or hollow. The modelling results are shown in Fig.6 for a time slice ($t = t_{max}$), corresponding to a maximum of $\beta_N = 3.3$ in high β_N , H-factor (Pulse No: 82794).

3. MHD, CONFINEMENT DEGRADATION AND RADIATION PEAKING

Benign kink 1/1 mode were observed in all quasi steady-state hybrid pulses with C-wall in good confinement phase ($\beta_N > 3$, $H > 1.1$). Kink modes are transformed to tearing-like modes in similar pulses with ILW. The amplitude of the $n = 1$ measured by magnetic probe, averaged over 400ms preceding t_{max} and t_1 , respectively, for all hybrid pulses with ILW is shown in Fig.7. The tearing mode erodes the temperature profiles. The confinement degradation correlates with formation of tearing modes. According to modelling and measurements, the q-profile is flat, close to 1 and may produce two or more $q = 1$ resonance surfaces in the core region. There is a correlation between tearing mode bursts and peaking of the radiation and soft X-ray emission profiles. Successive sawteeth flatten them (Fig.8). Enhanced radiation and sawteeth flatten T_e profiles, affecting the q-profile evolution in addition to the effect of peaked Z_{eff} . The radiation peaking due to MHD may be connected to the mechanism of the non-linear evolution of the tearing mode [2] in the presence of the poloidally non uniform distribution of heavy impurities. The W ions moves with the plasma frame as they have little thermal velocity compared to toroidal rotation velocity of the plasma. The W ions remain in tearing mode island for relatively long time. Vortex flows [1] cause redistribution of the W ions from the x-point region to 0- point in poloidal direction (yaxis in Fig.9). Tearing 3/2 and 4/3 modes have been typically observed in hybrid pulses with ILW with the largest confinement degradation.

SUMMARY AND CONCLUSIONS

The change in wall materials has affected both the plasma composition and the MHD phenomenology and these factors both modify the plasma performance. In particular, an accumulation of tungsten, tearing mode formation, radiation peaking and confinement degradation towards $H = 1$, have been observed in all high performance ($H > 1.1$) hybrid pulses with ILW. Maximum β_N and H-factor are reached typically in the first 1–2s of the high power phase. W is accumulated during this period in amount sufficient to modify later phase of the discharge. Statistically most common tearing 1/1 mode is connected to the specific features of the q-profile formed in the presence of the heavy impurities. Tearing mode formation correlates with confinement degradation. They often correlate with further peaking of the radiation and W concentration (Z_{eff}). In the later phase of the pulse the impurity accumulation accelerates due to the effects discussed in [C.Angioni this conference, Mantica this conference]. Future scenario development must, therefore, address the questions of MHD and impurity control in an integrated manner.

ACKNOWLEDGMENT

This work, supported by the European Communities under the contract of Association between EURATOM and CCFE, was carried out within the framework of the European Fusion Development Agreement. The views and opinions expressed herein do not necessarily reflect those of the European Commission. This work was also part-funded by the RCUK Energy Programme under grant EP/I501045.

REFERENCES

- [1]. ITER Physics Expert Groups on Confinement and Transport and Confinement Modelling and Database ITER Physics Basics Editors and ITER EDA 1999 Nuclear Fusion **39** 2175)
- [2]. Rutherford P.H, Physics of Fluids, **16**(1973) 1903

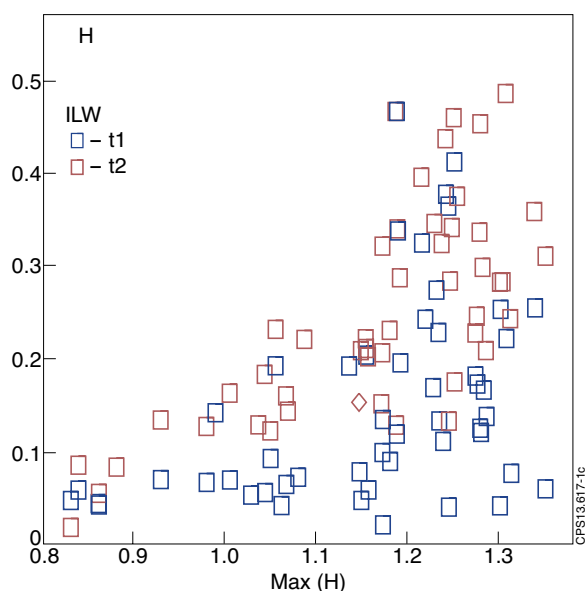


Figure 1: $\Delta H = H(t_{max}) - H(t_{1,2})$, $\max(H, \beta_N)$ reached at t_{max} , $t_1 = t_{max} + 0.6s$, $t_2 = 0.3s$ before the end of high power phase. Max reached β_N varies from 1.3 to 3.5 practically linear with $\max H$ 98y.

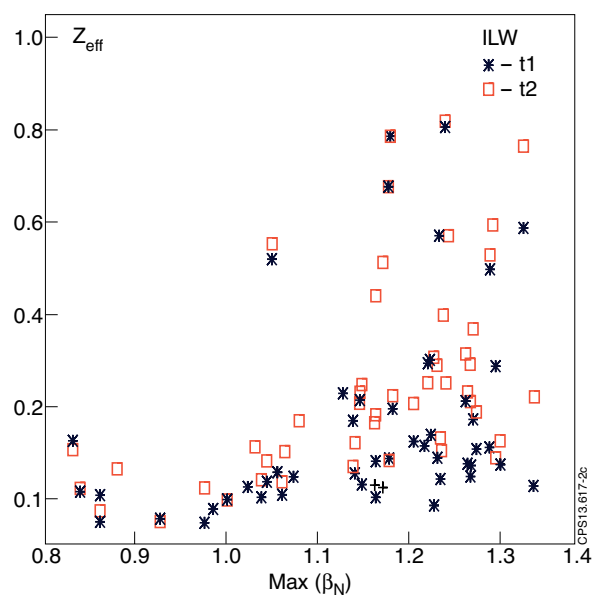


Figure 2: $\Delta(Z_{eff}) = Z_{eff}(t) - Z_{eff}(t_{max})$ in hybrid pulses with ILW. Parameters t_{max} , t_1 and t_2 are defined in Fig.1 caption.

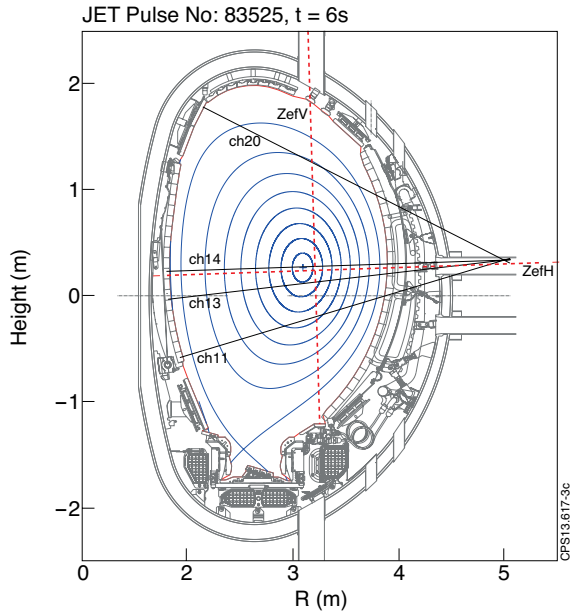


Figure 3: Cross section of JET plasma and observation lines for horizontal bolometer measurements (ch11-20) and vertical (Z_{effV}) and horizontal (Z_{effH}) lines for Z_{eff} measurements.

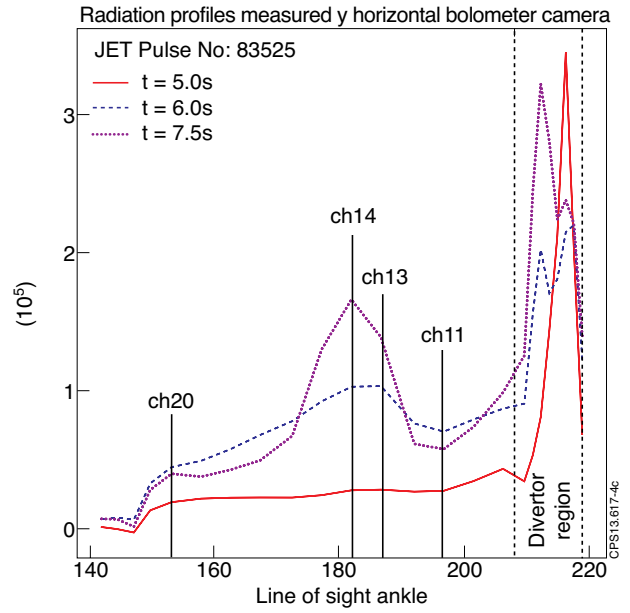


Figure 4: Profiles of bolometer measured radiation for successive times corresponding to beginning of NB heating, time of $\max \beta_N$ (t_{max}) and $t = t_{max} + 1.5s$. Position of marked lines of sight for ch11-20 are shown in Fig.3.

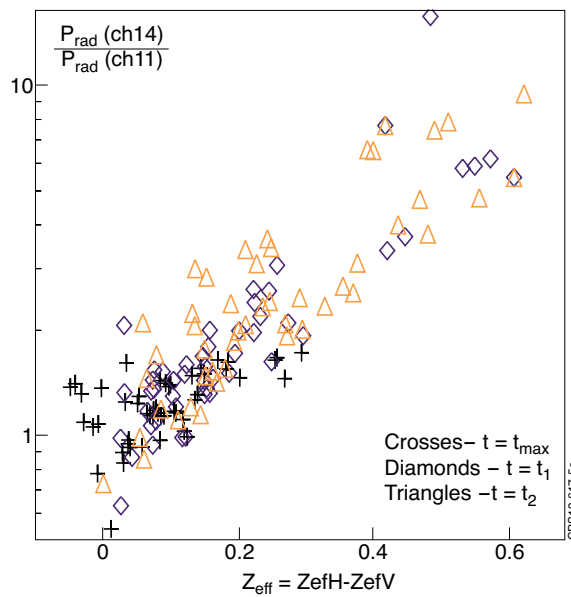


Figure 5: Correlation between radiation peaking $P_{rad}(ch14)/P_{rad}(ch11)$ and $Z_{effH} - Z_{effV}$.

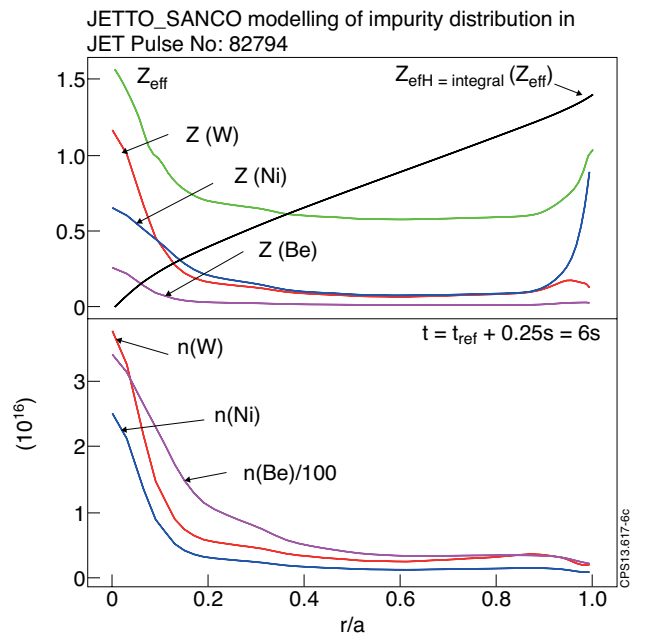


Figure 6: Profiles of Z_{eff} and densities of W, Ni, Be contributions, Pulse No: 82794, $t = 6s$.

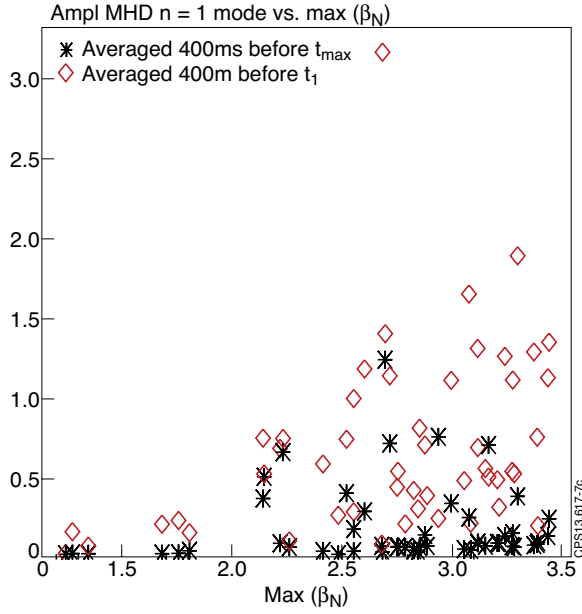


Figure 7: Amplitude of $n = 1$ mode measured by magnetic probe versus $\max(\beta_N)$.

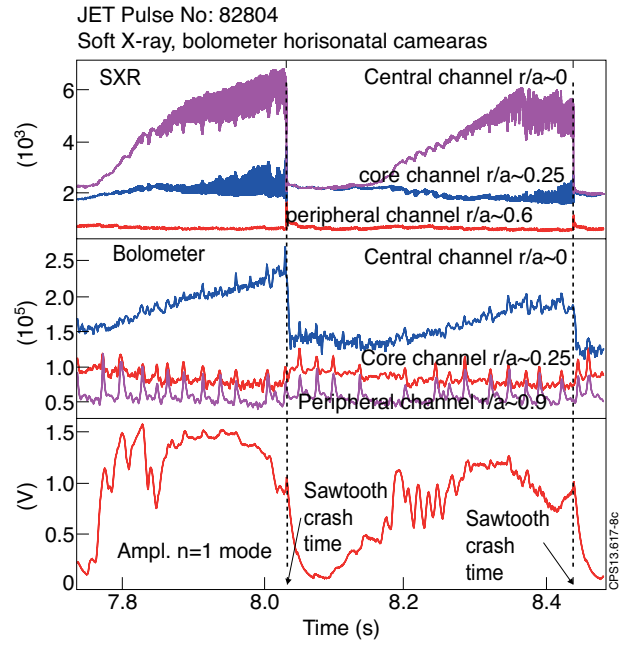


Figure 8: Variation of SXR and bolometer measured radiation and MHD $n=1$ mode amplitude. Pulse No: 82804.

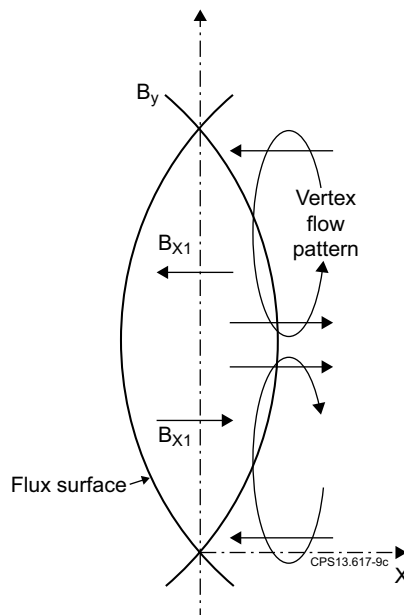


Figure 9: Tearing mode structure is produced by perturbation $B_y = B_y'x$. The vortex flow carries plasma into the magnetic island. Distribution of the heavy impurities is strongly inhomogeneous in the poloidal (y -axis) and radial (x -axis) directions. The influx of the heavy impurities caused by vortex flow causes peaking of the impurities near equatorial plane inside the vortex. See [2] for details of the island dynamics.